Pergamon

Bioorganic & Medicinal Chemistry 9 (2001) 2905–2919

BIOORGANIC & MEDICINAL CHEMISTRY

Tris-benzimidazole Derivatives: Design, Synthesis and DNA Sequence Recognition

Yu-Hua Ji,[a,†] Daniel Bur,[a] Walter Häsler,[a] Valérie Runtz Schmitt,[a] Arnulf Dorn,[a] Christian Bailly,[b,*] Michael J. Waring,[c] Remo Hochstrasser[a,d] and Werner Leupin[a,e,*]

[a]*F. Hoffmann-La Roche Ltd, Pharma Research Preclinical Gene Technologies and Infectious Diseases, CH-4070 Basel, Switzerland*

[b]*INSERM Unité 524 et Laboratoire de Pharmacologie Antitumorale du Centre Oscar Lambret, Place de Verdun, 59045 Lille, France*

[c]*Department of Pharmacology, University of Cambridge, Tennis Court Road, Cambridge CB2 1QJ, UK*

[d]*Biocentre of the University of Basel, Department of Biophysical Chemistry, Klingelbergstrasse 70, CH-4056 Basel, Switzerland*

[e]*Gymnasium Liestal, Abteilung Chemie, Friedensstrasse 20, CH-4410 Liestal, Switzerland*

Received 4 October 2000; accepted 10 May 2001

Abstract—Two tris-benzimidazole derivatives have been designed and synthesized based on the known structures of the bis-benzimidazole stain Hoechst 33258 complexed to short oligonucleotide duplexes derived from single crystal X-ray studies and from NMR. In both derivatives the phenol group has been replaced by a methoxy-phenyl substituent. Whereas one tris-benzimidazole carries a *N*-methyl-piperazine at the 6-position, the other one has this group replaced by a 2-amino-pyrrolidine ring. This latter substituent results in stronger DNA binding. The optimized synthesis of the drugs is described. The two tris-benzimidazoles exhibit high AT-base pair (bp) selectivity evident in footprinting experiments which show that five to six base pairs are protected by the tris-benzimidazoles as compared to four to five protected by the bis-benzimidazoles. The tris-benzimidazoles bind well to sequences like 5′-TAAAC, 5′-TTTAC and 5′-TTTAT, but it is also evident that they can bind weakly to sequences such as 5′-TATGTT-3′ where the continuity of an AT stretch is interrupted by a single G·C base pair.

Introduction

The dyes Hoechst 33342 and Hoechst 33258 (Fig. 1) are frequently used in cytometry to stain chromosomes in situ.[1,2] These two bis-benzimidazole compounds become brightly fluorescent when they bind to DNA. For a long time, it has been known that Hoechst 33258 binds specifically to AT-rich sequences in DNA.[3–10] A variety of NMR and X-ray crystal structures of Hoechst 33258 bound to different oligonucleotide duplexes have been published.[11–19] Collectively, these structural studies reveal that the drug fits snugly into the minor groove of the double helix, covering a run of four contiguous A·T base pairs (bp). The Hoechst 33258–DNA interaction appear to be stabilized by several H-bonding and van der Waals contacts[20] but in fact these molecular forces are believed to contribute little to overall binding affinity.[21] The hydrophobic transfer of ligand from solution on to its DNA binding sites is more likely to represent the main driving force for the complex formation.[21] There is no doubt, however, that the width of the minor groove of the double helix is a major determinant of Hoechst 33258 binding to particular AT stretches. Interactions with the walls of the minor groove furnish the most important contributions to binding of benzimidazole derivatives.[22]

The high affinity of Hoechst 33258 for AT-rich sequences in DNA, together with its interesting anti-microbial properties, have encouraged the design of analogues better able to target specific sites in DNA. A number of bis-benzimidazoles equipped with various side chains have been reported. For example, the replacement of the terminal piperazine ring with an amidinium, an imidazoline or a tetrahydropyridinium group reinforces significantly the affinity of the drug for AT stretches.[23–25] Substituting a small group for the bulky

*Corresponding author. Tel.: +33-320-169218; e-mail: ,
†Present address: Advanced Medicine Inc., 901 Gateway Blvd, South San Francisco, CA 94080, USA.

0968-0896/01/$ - see front matter
PII: S0968-0896(01)00170-5

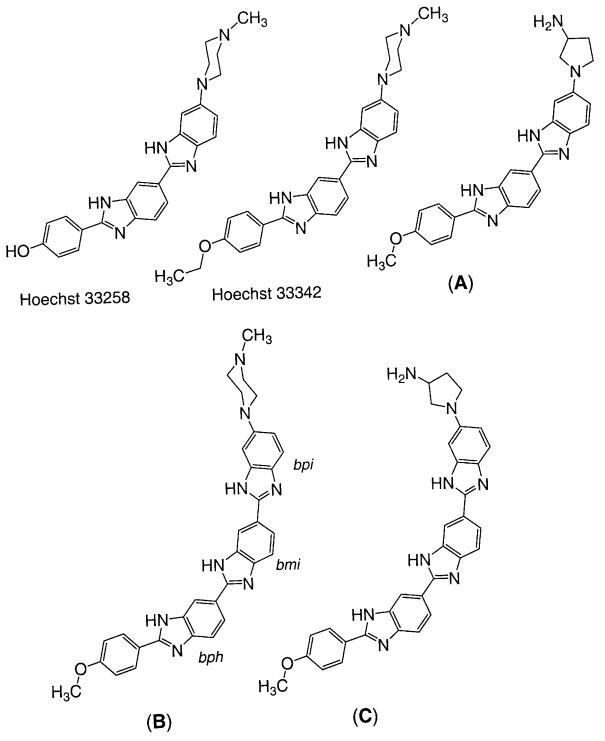

Figure 1. Structures of the DNA ligands used in this study.

piperazine results in a narrower groove at the 3′ end of the drug binding site and therefore a smaller perturbation of groove width.[23] At the other end of the molecule, the relocation of the phenolic hydroxyl group from the *para* to the *meta* position (*meta*-Hoechst) has relatively little impact on the sequence-selectivity of the interaction with DNA.[26,27] The central part of the parent molecule has also been modified with the aim of designing compounds capable of recognizing GC-containing sequences. In some cases, the replacement of one or both of the benzimidazole units with another heterocycle (e.g., benzoxazole, pyridoimidazole, etc.) has produced GC-tolerant compounds[28–31] but not really produced highly GC-selective analogues.

Inspection of NMR and X-ray structures of Hoechst 33258 bound to d(CGCGAATTCGCG)$_2$ revealed that the drug is positioned with the phenol ring situated between base pairs involving G(4) and T(5) and the methyl-piperazine ring between base pairs involving T(7) and T(8). A different molecular architecture has been reported when the drug is bound to the dodecanucleotide d(CGCAAATTTGCG)$_2$. In this case, Hoechst 33258 was found to bind to the 5′-ATTTG sequence in a unique orientation.[19,32] In other words, Hoechst 33258 was displaced by one base pair compared to the structures determined previously for this drug with the sequence d(CGCGAATTGCGC)$_2$. Consideration of this fact led us to propose elongating Hoechst 33258 by one benzimidazole unit to yield tris-benzimidazole derivatives capable of covering more base pairs, and perhaps to improve affinity for a longer A/T-rich tract of DNA or to change the sequence specificity. Another approach to improve selectivity and binding strength of ligands derived from Hoechst 33258 was recently employed using a tripyrrole peptide–Hoechst conjugate.[33]

The structures determined for Hoechst 33258 bound to d(CGCAAATTTGCG)$_2$ were used to model the tris-benzimidazole derivative **B** which is one unit longer than the parent molecule (Fig. 1). According to computational studies with our in-house modeling package MOLOC[34] (check also the MOLOC homepage under http://www.moloc.ch), compound **B** would cover six base pairs and fit snugly into the narrow minor groove of the A3T3 stretch. All three benzimidazole NHs would engage in H-bonds to either O2 of thymines or N3 of adenines. While benzimidazoles *bpi* and *bmi* prefer to contact O(2) of T(8) and O(2) of T(7) in the 5′ strand, respectively, benzimidazole *bph* contacts O(2) of T one base pair upstream in the 3′-strand. Other H-bond patterns for **B** were examined but they all showed higher overall energy. Dihedral angles of 31 and 39° were measured between benzimidazole units. The 4-*N*-methyl-piperazine ring is located between the base pairs involving T(9) and G(10) while the methoxy-phenyl moiety covers base pairs four and five. A number of possible replacements for the basic 4-*N*-methyl-piperazine ring were modelled among which a 3-NH_2-pyrrolidine might gave the best results, corresponding to molecule **C** (Fig. 1). The computer analysis suggested that the protonated NH_2 group could form two H-bonds to DNA compared to only one with the charged 4-*N*-methyl-piperazine ring. The smaller five-membered ring fits deeper into the narrow minor groove than the more voluminous six-membered ring, thereby decreasing the water accessible hydrophobic surface of the buried ligand.

The tris-benzimidazole **B** possessing a piperazine terminal ring can be directly compared with Hoechst 33342 and Hoechst 33258. By contrast, the DNA-binding properties of the tris-benzimidazole **C** have to be examined relative to a related bis-benzimidazole derivative **A** bearing the same aminopyrrolidine terminal group (Fig. 1). Here, we report the synthesis of the bis- and tris-benzimidazoles **A**, **B** and **C**. Their capacity to recognize specific sequences in DNA has been investigated using deoxyribunuclease I (DNase I) footprinting methodology, with several different DNA restriction fragments as targets or substrates.

Results

Chemistry

The synthesis of bis-benzimidazole derivatives was carried out basically according to the method reported by Lown et al.[35] The benzimidazole **3** resulted from the condensation of 4-substituted *o*-arylenediamine and anisaldehyde. The ester function of **3** was converted to aldehyde **5** by reduction and oxidation (Scheme 1, method A). The later was coupled with 4-aminosubstituted *o*-arylenediamino **11** or **12** to afford the bis-benzimidazole derivatives. However, we introduced two important modifications. The first one concerns the

synthesis of aldehyde **5**. Although its synthesis by method A in good yield was reported, we always obtained variable yields of both alcohol **4** and aldehyde **5** especially on the large scale. This was probably due to the poor solubility of these compounds in the reaction solvents such as THF and CH_2Cl_2. Furthermore, during the reduction of the ester to alcohol **4**, the further reduced by-product 5-methylbenzimidazole was obtained with prolonged reaction time under reflux. The reduction of *N*-methoxy methylamide to aldehyde has been reported.[36] Therefore, the synthetic route for aldehyde **5** was improved as follows (Scheme 1, method B): 3,4-dinitrobenzoic acid was transformed to amide **6**, which was hydrogenated to the corresponding diamine and subsequently condensed with aldehyde to yield benzimidazole **7**. Treatment of compound **7** with $LiAlH_4$ in THF afforded aldehyde **5** in high yield.

The second modification concerns the benzimidazole ring formation. Heating of an equimolar *o*-arylenediamine and an aldehyde in nitrobenzene has usually been adopted as a convenient and widely applicable route for the construction of the benzimidazole unit. The reaction consists of two steps: the Schiff base formation and the oxidative cyclization. Nitrobenzene is used as solvent as well as oxidant. This method has many advantages over the condensation of *o*-arylenediamine and arylcarboxylic acid or their derivatives such as imidate ester, chloride and anhydrides[37,38] in strongly acidic conditions. However, using this method the reaction did not always proceed sufficiently smoothly; it required relatively high temperatures together with long reaction times, and the desired benzimidazole derivative was obtained in variable yields, and in some cases the by-products such as Schiff base and dihydrobenzimidazole derivative were also isolated. The daily use of nitrobenzene as a solvent was also not convenient in the laboratory. The dehydrogenating capacity of bisulfite has been demonstrated in the condensation of 1,8-diaminonaphthalene and aldehyde to 2-substituted 1H-pyrimidines.[39,40] However, there is no previous report on the synthesis of bis-benzimidazole derivatives utilizing bisulfite as an oxidizing reagent. We therefore explored the possibility of constructing benzimidazole unit from *o*-arylenediamine and aldehyde in the presence of bisulfite. The condensation was carried out in ethanol. After hydrogenation of *o*-dinitroarylene to the corresponding diamine an aqueous solution of sodium pyrosulfite, which generated bisulfite in situ, was introduced directly in to the reaction mixture. Following addition of the appropriate aldehyde, the mixture was heated under reflux for 4 h to give the desired mono, bis- or tris-benzimidazole derivatives, respectively, in high yield. This procedure is easy to handle and offers the possibility of accomplishing the hydrogenation of dinitro to diamine and the subsequent condensation with aldehyde in a one-pot reaction. Therefore, bis-benzimidazole aldehyde derivative **10** was easily prepared by using these modified procedures (Scheme 2). 3,4-Diaminobenzoic acid was coupled with

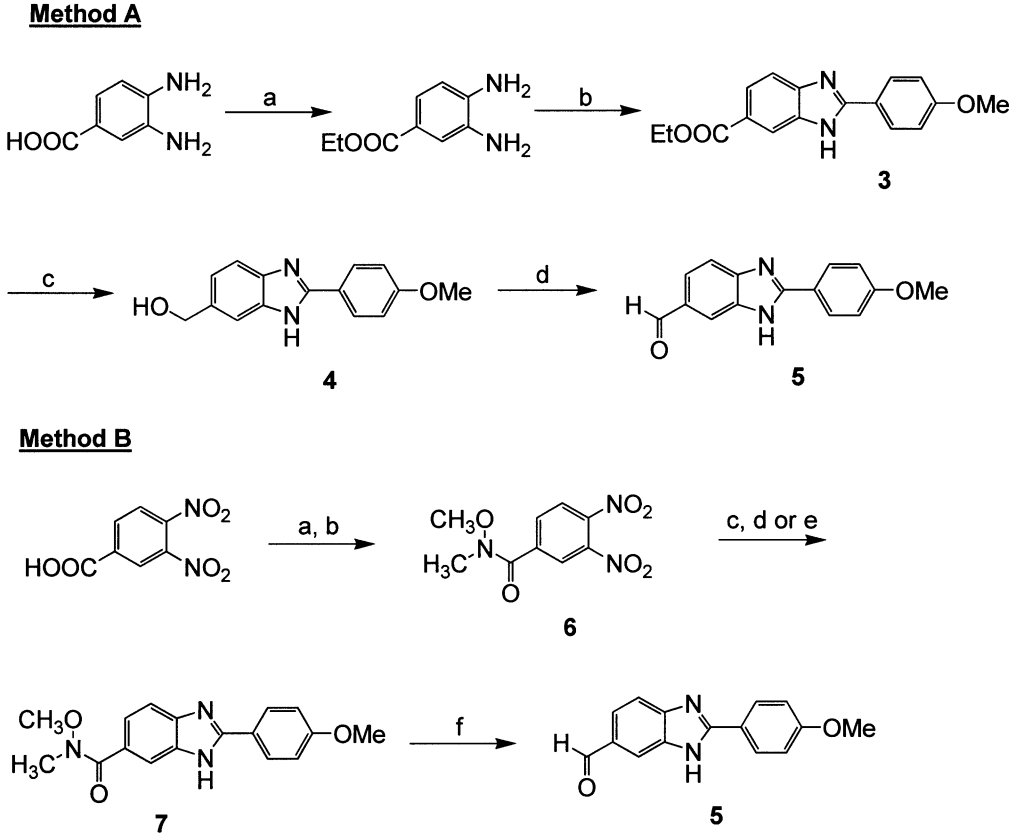

Scheme 1. (A) (a) HCl/EtOH; (b) 4-methoxybenzaldehyde, $PhNO_2$, 140 °C; (c) $LiAlH_4$, THF/dioxane, reflux; (d) PCC, pyridine/CH_2Cl_2 or MnO_2, DMF/CH_2Cl_2; (B) (a) $SOCl_2$, 80 °C; (b) CH_3ONHCH_3·HCl, Py, CH_2Cl_2, rt; (c) H_2, 5% Pd/C, EtOH, rt; (d) 4-methoxybenzaldehyde, $PhNO_2$, 140 °C; (e) 4-methoxybenzaldehyde, $Na_2S_2O_5$, EtOH/H_2O, reflux; (f) $LiAlH_4$, THF, 0 °C→rt.

monobenzimidazole aldehyde **5** in the presence of bisulfite in ethanol and water to give bisbenzimidazole carboxylic acid derivative **8**. Then the acid function was converted to amide **9**, which was subsequently reduced to bisbenzimidazole aldehyde **10**.

In conclusion, the convergent synthesis of titled bis- and tris-benzimidazoles is as follows: 5-chloro-2-nitroaniline was treated with the appropriate cyclic secondary amine in DMA to yield the 5-aminosubstituted nitroaniline. Catalytic hydrogenation of the latter to the corresponding 4-substituted *o*-phenylenediamine was followed by condensation with aldehyde **5** or **10**, in the presence of aqueous sodium pyrosulfite, to furnish bis- and tris-benzimidazoles, compounds **1b**, **2a**, **2b**, respectively (Scheme 2).

DNA binding strength

We measured the ability of the bis- and tris-benzimidazole derivatives to alter the thermal denaturation profile of calf thymus DNA. Under the experimental conditions used (16 mM Na^+), the helix-to-coil transition occurs at 60 °C in the absence of drugs. The T_m is shifted to higher temperature with all five drugs but the extent of stabilization differs significantly for the tris-benzimidazoles compared to the bis-benzimidazoles. As represented in Figure 2, at a drug–DNA (P) ratio of 0.25, a ΔT_m value (T_m complex $- T_m$ DNA) of 12 °C was measured with Hoechst 33258 whereas the ΔT_m reaches 24 °C with compound **B**. A much larger ΔT_m value was also measured with the other tris-benzimidazole derivative **C** compared to the corresponding bis-benzimidazole **A** ($\Delta T_m = 14$ and 25 °C for **A** and **C**, respectively). We can therefore conclude that the additional benzimidazole unit reinforces the interaction of the drugs with DNA. These T_m data are in agreement with the footprinting data reported below.

DNA binding mode

To characterize the mode of binding to DNA, linear dichroism (LD) spectra of the bis-benzimidazole **A** (known as a minor groove binder) and the two tris-benzimidazoles **B** and **C** were measured in the presence of calf thymus DNA, using a simple, easy to handle and inexpensive Couette cell for flow oriented linear dichroism.[41] All three compounds exhibit a spectral region (at $\lambda > 330$ nm) where DNA does not absorb the light thus allowing the study of the mode of binding by this method. The absorption and LD spectra of compounds **B** and **C** complexed with calf thymus DNA are presented

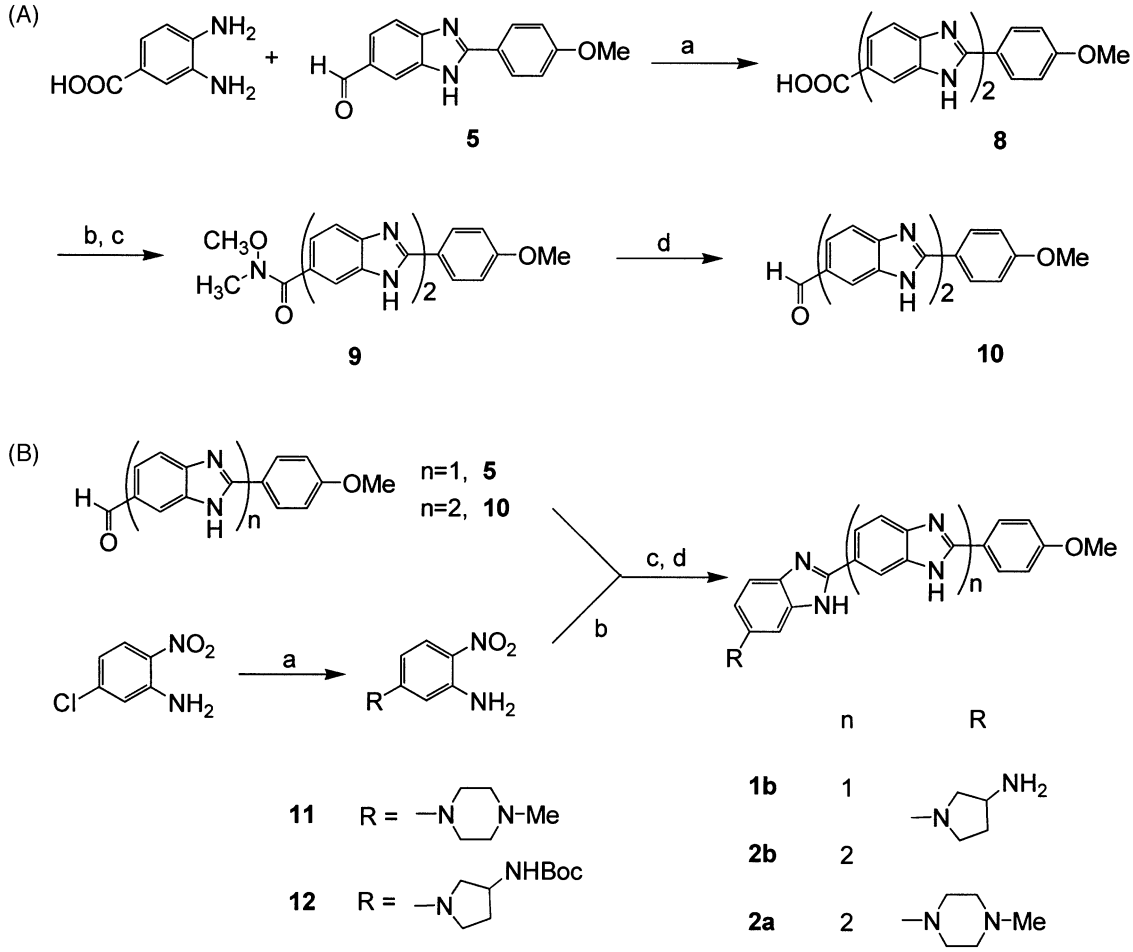

Scheme 2. (A) (a) $Na_2S_2O_5$, $EtOH/H_2O$, reflux; (b) $SOCl_2$, 80 °C; (c) $CH_3ONHCH_3 \cdot HCl$, Py, CH_2Cl_2, rt; (d) $LiAlH_4$, THF, 0 °C → rt; (B) (a) 3-BocNH-pyrolidine or 4-*N*-methylpiperazine, K_2CO_3, DMF, 90 °C; (b) H_2, 5% Pd/C, EtOH, rt; (c) $Na_2S_2O_5$, $EtOH/H_2O$, reflux; (d) only for compounds **1b** and **2b**: TFA/CH_2Cl_2.

in Figure 3. In both cases, the LD is negative in the DNA absorption band centered at 260 nm, indicative an orientation of the base pairs perpendicular to the long axis of the biopolymer. In contrast, positive LD signals in the absorption bands of the ligands at wavelengths higher than 330 nm (where DNA does not absorb) are observed with compounds **B** and **C** (Fig. 3), as well as with compound **A** (spectrum not shown). These spectra indicate that in all three cases the orientation of the bis- or tris-benzimidazole chromophores is colinear to the orientation of the DNA helix. In other words, compounds **A**, **B** and **C** do not intercalate between the DNA base pairs but bind to one of the grooves of the double stranded DNA helix, most likely the minor groove as is known to be the case with Hoechst 33258 and related bis-benzimidazoles including compound **A**. The experimental finding of groove binding of the two tris-benzimidazoles **B** and **C** has in the meantime been verified by X-ray studies of **C** complexed to the oligonucleotide duplexes $d(CGCAAATTTGCG)_2$[27] and to the non-self-complementary dodecamer DNA duplex d(CG[5BrC]A-TAT-TTGCG)•d(CGCAAATATGCG).[42] Our observations differ from those reported[43] with the tris-benzimidazole derivative 5PTB which exhibits both intercalative and minor groove binding properties. In our experiments, the two tris-benzimidazole derivatives behave as pure groove binders.

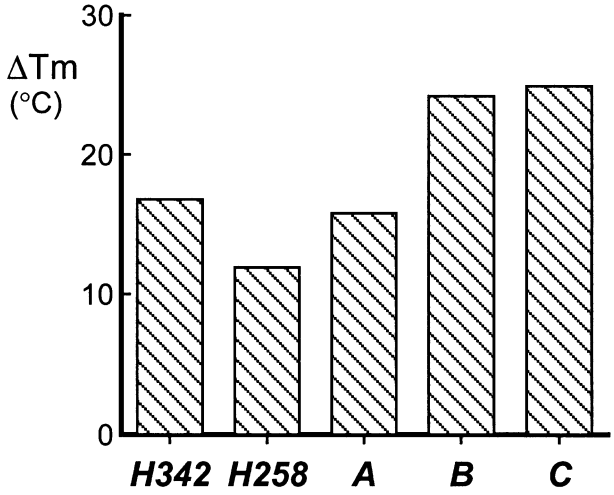

Figure 2. Variation of the melting temperatures (ΔT_m) for calf thymus DNA in the presence of the bis- and tris-benzimidazoles. T_m measurements were performed in BPE buffer pH 7.1 (6 mM Na_2HPO_4, 2 mM $Na_2H_2PO_4$, 1 mM EDTA) using 20 μM DNA and 5 μM drug, in 1 mL quartz cuvettes at 260 nm with a heating rate of 1 °C/min.

DNA sequence recognition

DNase I footprinting experiments were carried out using three DNA restriction fragments chosen for their diverse arrangements of base pairs. With each fragment, the products of digestion by DNase I in the absence and presence of the test drugs were resolved by polyacrylamide gel electrophoresis. Typical autoradiograms are illustrated in Figures 4 and 5. Strong differences between the control lanes and those for the tested drugs can easily be seen. Areas of decreased intensity (i.e., footprints) in ligand-containing lanes relative to ligand-free lanes reflect cleavage inhibition due to ligand bound to specific nucleotide sequences, and densitometric analysis of the different patterns permits estimation of the

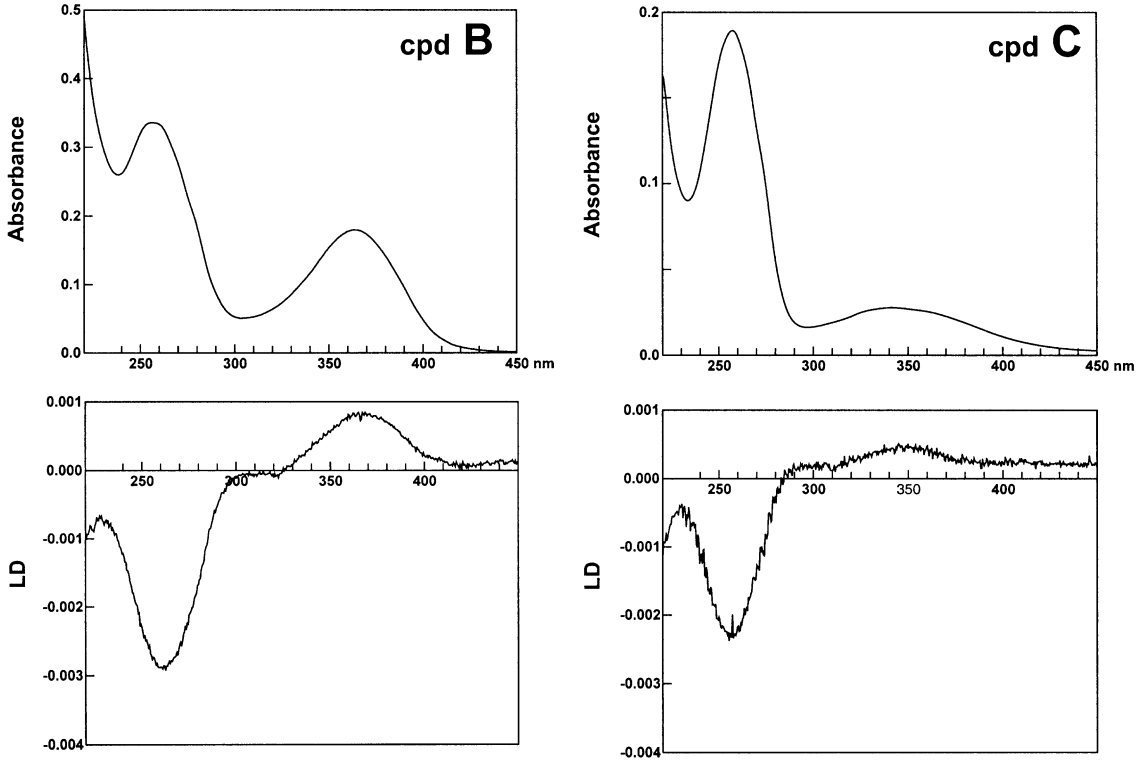

Figure 3. Absorption (upper panel) and linear dichroism (lower panel) spectra of compounds **B** and **C** complexed to calf thymus DNA (average length approx. 2500 base pairs) in 50 mM phosphate buffer of pH 7.0, 100 mM NaCl and 0.1% NaN_3.

location and relative strength of binding at particular DNA sites. Figure 6 shows a selection of differential cleavage plots determined with the three DNA fragments in the presence of the bis-benzimidazole **A** and the tris-benzimidazole derivatives **B** and **C**. Experiments were also performed with Hoechst 33258 and Hoechst 33342 for comparative purposes. The dips in these plots (negative values) indicate sites of protection from DNase I cleavage, whereas peaks (positive values) indicate regions of drug-induced enhancement of nuclease cleavage. We will consider the results obtained with each fragment in turn.

The 117 bp DNA fragment (Fig. 4, panel B and Fig. 6, panel a). Four major sites of drug protection can be discerned around nucleotide positions *25*, *43*, *64* and *85*. These protected zones each extend for about eight nucleotides. All four are situated in AT-rich sequences of the DNA. Adjoining these protected sites are regions where the rate of DNase I cutting is significantly enhanced relative to the control. These regions of relatively enhanced cleavage always occur in GC-rich sequences as for example at positions *34–38* and *71–74* in this DNA. The densitometric analysis was necessarily limited to the regions of the gel where the bands are well separated: at first sight, the patterns of enhancement and protection between nucleotide positions *26* and *78* appear virtually identical for the three test compounds **A**, **B** and **C** and for the two control drugs Hoechst 33258 and Hoechst 33342. However, closer inspection of the gels reveals an interesting difference between the bis and the tris-benzimidazole compounds. The sites protected from DNase I cleavage by the tris-benzimidazoles **B** and **C** are often 1–2 bp longer than the corresponding sites detected with the bis-benzimidazoles. This is clearly visible between positions *40* and *46* of this DNA fragment, as shown in Figure 7. At this site, the sequence 3′-CAAAA is protected from cleavage by DNaseI in the presence of Hoechst 33258, Hoechst 33342 and compound **A**. With the tris-benzimidazoles **B** and **C**, it is obvious that the binding site is one base pair longer and encompasses the sequence 3′-CAAAAT. The inference is clear that the longer footprints obtained with tris-benzimidazoles compared to the bis-benzimidazoles reflect the binding specificity of the third benzimidazole group present in compounds **B** and **C**. It is also worth noting that the tris-benzimidazole **C** seems to produce stronger protection from DNase I cutting than does Hoechst 33258 or the other test drugs. This can be seen in the differential cleavage plots in Figure 6a as well as on the gel in Figure 4a around position *85* where the footprint produced by compound **C** is substantially more pronounced than those produced by the other drugs.

The *tyr*T DNA fragment (Fig. 4, panel A and Fig. 6, panel b). As with the 117-mer fragment, the sites protected by the test drugs **A**, **B** and **C** coincide with those protected by the control drugs Hoechst 33342 and Hoechst 33258. All produce strong protection around positions *29*, *44* and *82* of the DNA. The *tyr*T fragment has been used previously to map the binding sites of Hoechst 33258,[3] and the sites observed here are identical to those previously reported with this piece of DNA. The most significant observation is that, consistent with the finding on the 117-mer DNA fragment, the sequences protected from DNase I cleavage by the tris-benzimidazoles **B** and **C** are 1–2 bp longer than those protected by Hoechst 33258. A conspicuous example occurs in the A-tract at positions *48–52*. The 5′-most adenine residue of the A run (i.e., position A*52*) is protected from nuclease attack by compounds **B** and **C** whereas this adenine remains fully accessible to the enzyme in the presence of Hoechst 33258 and the related bis-benzimidazole derivatives. The same observation can be made for the adenine at position *26* (i.e., protection by **B** and **C** but unimpeded cleavage with Hoechst 33258). Therefore, this second set of footprinting experiments reinforces the previous conclusions that (i) the test compounds are AT-specific groove binders and (ii) the DNase I protected sites are slightly longer with the tris-benzimidazoles compared to the bis-benzimidazoles. All the experiments agree that the three benzimidazole units of compounds **B** and **C** bind firmly to DNA and engage in specific contact with A•T base pairs.

The 178bp DNA fragment (Fig. 5 and Fig. 6, panel c). With this fragment the footprinting experiments were carried out using a 5-fold lower drug concentration than the experiments with the 117-mer and the *tyr*T DNA. The differential cleavage plots obtained for Hoechst 33258 and the bis-benzimidazole derivative **A** superimpose quite well, showing that compound **A** selects AT-rich sites very similar to those bound by Hoechst 33258. The replacement of the piperidine terminal group of Hoechst with a pyrrolidine group evidently has little effect on DNA sequence recognition. Interestingly, under the conditions used here we can observe significant differences between the bis- and the tris-benzimidazole compounds. Both the gel and the differential cleavage plots concur that several sequences are protected from nuclease attack by the tris-benzimidazoles **B** and **C** but not by the bis-benzimidazole derivatives. This is particularly noticeable at the AT-rich sequence between nucleotide positions *80* and *91* where, allowing for the usual 3′-shift by 2 bp due to the bias introduced by the enzyme cutting in the minor groove, we can locate binding sites for compounds **B** and **C** at the sequences 3′-CATTT *87–91* and 3′-TATTT *80–84*. In addition, the existence of two more binding sites can be discerned from the gaps in the gels near positions *105* and *120* (Fig. 5). They lie beyond the range accessible to densitometry but are clearly visible at the top of the autoradiograph. At higher concentrations ($\geq 10\,\mu M$) the bis-benzimidazole compounds also produce footprints at the same sequences (data not shown). These observations again suggest that the tris-benzimidazoles are endowed with a higher affinity for DNA compared to the bis-benzimidazole compounds. Interesting also is the observation that a weak site exists around the sequence 5′-TATGTT *62–67*, detectable only with the tris-benzimidazoles, indicating that drugs **B** and **C** can accept a sequence containing a G•C base pair as a secondary binding site, presumably with lower affinity. As observed with the 117-mer and the *tyr*T fragment, regions of the 178 bp DNA can be seen where nuclease

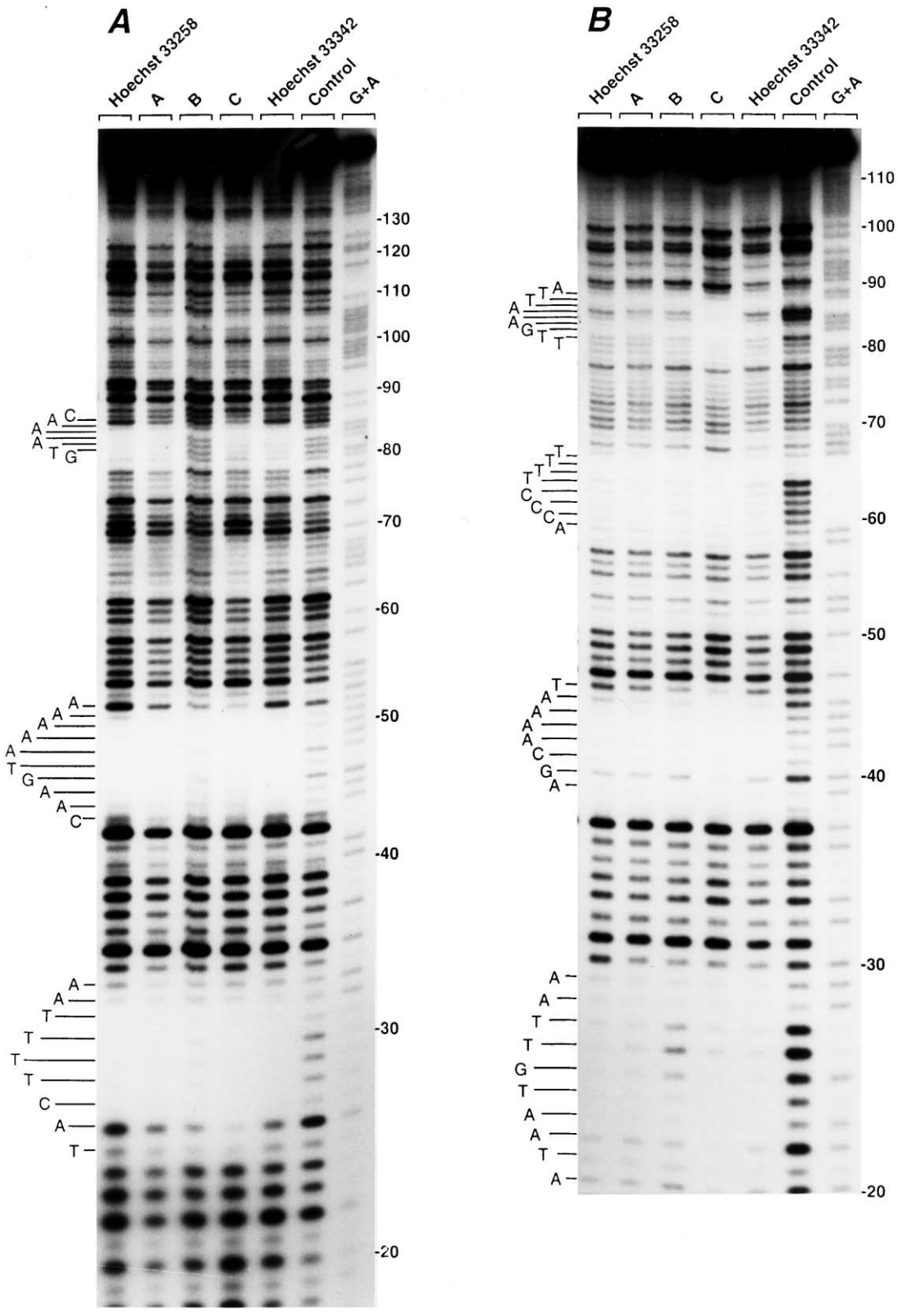

Figure 4. DNase I footprinting of Hoechst 33258, Hoechst 33342 and compounds **A**, **B**, and **C** (10 μM each) on the 160 bp *Eco*RI–*Ava*I *tyr*T fragment cut out from plasmid pKMΔ-98 (panel A) and the *Eco*RI–*Pvu*II 117 bp fragment cut out from plasmid pBS (panel B). In both cases, the duplex was 3′-end labeled at the *Eco*RI site with [α-^{32}P]dATP in the presence of AMV reverse transcriptase. The cleavage products of the DNase I digestion were resolved on an 8% polyacrylamide gel containing 8 M urea. Tracks labeled Control contained no drug. Lanes labeled G + A represent formic acid-piperidine markers track specific for purines. The sequences on the left side indicate the sites protected from DNase I cleavage. Numbers at the right side of the gels refer to the numbering scheme used in Figure 6 (panels a and b).

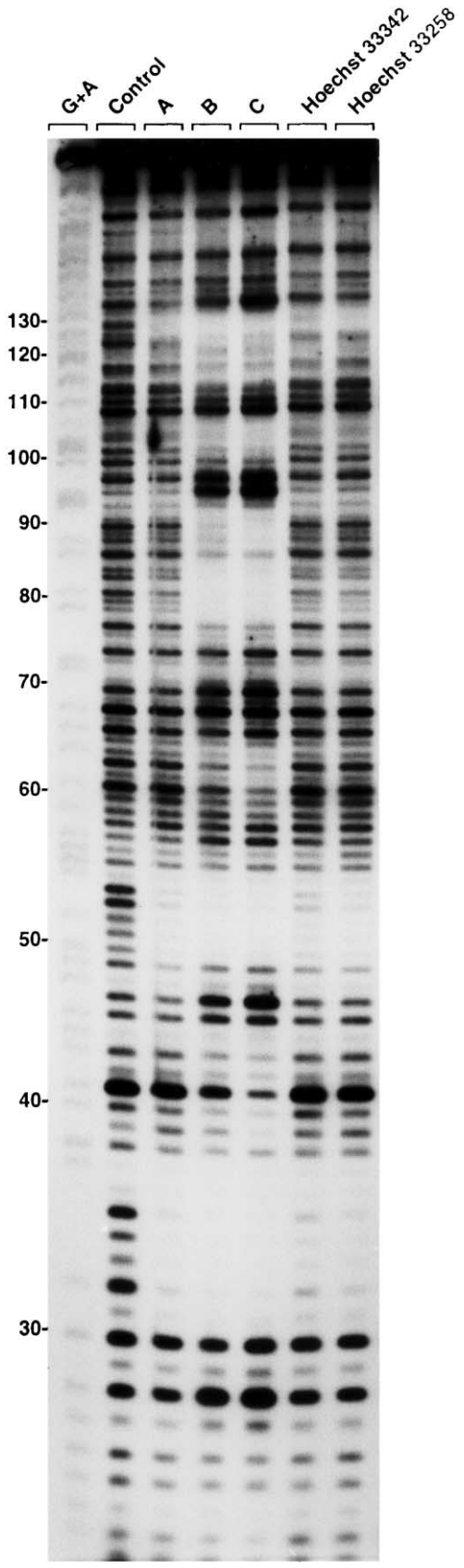

Figure 5. DNase I footprinting of Hoechst 33258, Hoechst 33342 and compounds **A**, **B**, and **C** (2 μM each) on the 178 bp *Eco*RI–*Pvu*II fragment cut out from plasmid pUC12. Numbers at the side of the gels refer to the numbering scheme used in Figure 6 (panel c). Other details as for Figure 4.

cutting is enhanced in the presence of the test drugs compared with the control. Good examples (Fig. 6c) occur at positions *44–47* (3′-GGCG) and *71–75* (3′-CGGCC), that is in regions containing contiguous G•C base pairs. There is no doubt that binding of these drugs to pure GC sequences is strongly disfavored.

Discussion

Sequence specific recognition of the minor groove of DNA by low-molecular weight synthetic ligands is a fast-growing field of research.[44,45] The ligands of interest are derived from different classes of chemical compounds, and generally represent elongated molecules containing repeating chemical entities capable of forming hydrogen bonds with building blocks of the DNA, acting both as hydrogen bond donors as well as hydrogen bond acceptors. Based on the high propensity of Hoechst 33258 to bind to AT-rich sequences, particularly those containing four contiguous A•T base pairs,[46] we decided to add one more benzimidazole unit resulting in tris-benzimidazole derivatives that should cover longer sites on DNA. According to modelling studies, the incorporation of a third benzimidazole unit should in principle allow the recognition of a specific DNA sequence that is about 6 bp long. The footprinting experiments presented here provide clear data that vindicate the hypothesis fully. The results in Figure 5 show clearly that the AT binding sites occupied by compounds **B** and **C** are 1–2 bp longer than those occupied by their bis-benzimidazole counterparts. The T_m and footprinting experiments concur that the tris-benzimidazoles **B** and **C** interact more tightly with DNA than do the equivalent bis-benzimidazoles. All this is consistent with the predictions of our modelling studies.

There exists a general consensus that DNase I detects sequence–specific interactions between drugs and DNA with high sensitivity but tends to overestimate the size of the binding sites. This view has its origins in footprinting investigations where the size of drug binding sites detected with DNase I was compared to those detected with other probes, mostly metal chelates.[47,48] The elucidation of the crystal structure of a DNase I–DNA complex[49,50] has substantiated this belief: in binding to DNA, the enzyme engages in contacts with two phosphates on either side of the cleaved bond and two phosphates on the other strand across the minor groove, opposite the phosphates contacted on the 5′ side of the cleaved bond. Nevertheless, the results reported here show that DNase I can sensitively detect the drug–DNA interaction and also accurately define the region that is contacted by the drug. From a technical point of view, the footprinting data reported here confirm our previous observations[51] that the supposed inability of DNase I to depict the exact position of ligand binding is not always justified. If it is optimally used (under single hit kinetic conditions), there is no doubt that DNase I can provide a very sensitive and accurate estimation of drug binding site sizes, at least for minor groove-binders as studied here.

The tris-benzimidazole **B** bearing a piperazine terminal group has not been described before, but a similar compound containing an aminopyrrolidine terminal group (tris-benzimidazole **C**) has been the subject of a crystallographic study: Neidle and co-workers solved the structure of a complex formed between the self-complementary dodecamer d(CGCAAATTTGCG)$_2$ and compound **C**, named TRIBIZ.[27] In the crystal

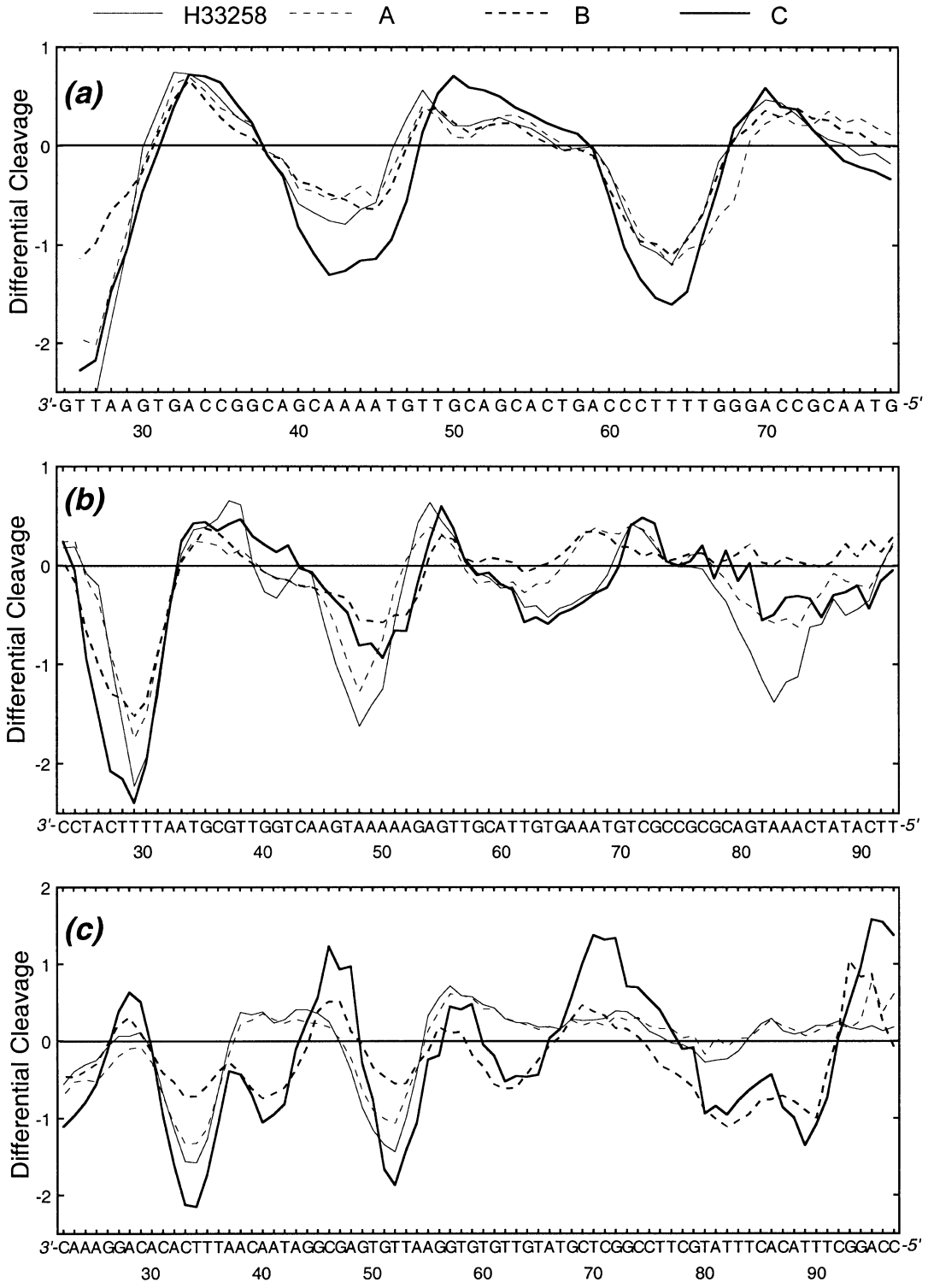

Figure 6. Differential cleavage plots comparing the susceptibility of the 117-mer (a), 160-mer *tyr*T (b), and 178-mer (c) fragments to DNase I cutting in the presence of the test drugs **A**, **B** and **C** and Hoechst 33258. The plots were measured by densitometry using phosphorimages of the gels shown in Figures 4 and 5. Negative differential cleavage corresponds to a ligand-protected site and positive differential cleavage occurs where the nucleolytic cutting is enhanced. Vertical scales are in units of ln(fa)−ln(fc), where fa is the fractional cleavage at any bond in the presence of the drug and fc is the fractional cleavage of the same bond in the control, given a similar extent of digestion in both cases. Each line drawn represents a three-bond running average of individual data points, calculated by averaging the value of ln(fa)−ln(fc) at any bond with those of its two nearest neighbors.

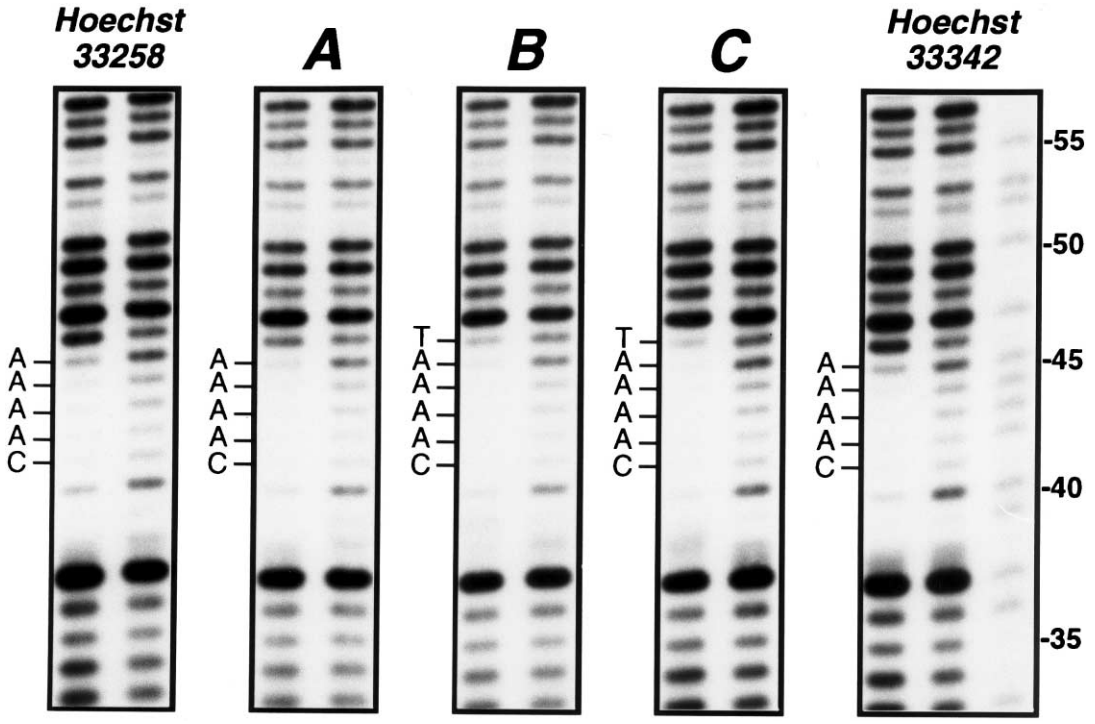

Figure 7. Portions of autoradiographs showing DNase I footprinting of the drugs on the 3′-end labeled 117 bp *Eco*RI-*Pvu*II restriction fragment. Each pair of lanes corresponds to cleavage by the enzyme in the presence (left) and absence (right) of the test drug. The third lane in the panel corresponding to Hoechst 33342 shows the G + A sequencing markers. The scale on the right side of this panel refers to the numbering of the DNA fragment as represented in Figure 6. Other details as for Figure 4.

structure, the drug **C** occupies the central AAATTT region of the duplex. The recognition site for the tris-benzimidazole drug **C** is best described by the sequence 5′-CAAATTTG whereas the bis-benzimidazole Hoechst 33258 interacts with the sequence 5′-ATTTG in its complex with the same dodecamer.[52] It is gratifying that our footprinting results agree with these data, for example showing that the binding sites for the tris-benzimidazole **B** are longer than those for the bis-benzimidazole. But the DNase I experiments reveal additionally that the ligand can accommodate binding sites that do not merely contain six contiguous A•T base pairs. For example, the sequence 5′-TTTACACTTTAT around position 85 on the 178-mer fragment (Fig. 6c) provides a privileged binding site for the tris-benzimidazole. The differential cleavage plots in Figure 6 show that the binding sites for the drugs **A**, **B** and **C** can contain a minimum of 4 A•T base pairs.

Experimental

Chemistry

All the chemicals were purchased from Fluka or Aldrich. Reagent grade solvents, purchased from Fluka, were used without further purification. Evaporation means removal of solvent by using a Büchi rotary evaporator at 35–50 °C in vacuo. Normal phase silica gel used for flash chromatography was Kieselgel-60 (230–400 mesh) or Florisil (60–100 mesh). Reverse-phase silica gel used was Opti-up RP 18. For HPLC, Lichrospher® 60 RP-select B (5 μm) column was used. TLC plates coated with silica gel 60 F_{254} (Merck) were used and detected by UV (254 nm), by treatment with concentrated H_2SO_4 and then 5% vaniline solution in ethanol followed by heating. ^{1}H NMR spectra were taken on Bruker AC 250 (250 MHz) or Bruker AM 400 (400 MHz), with TMS as internal reference and are expressed in δ units (parts per million). Mass pectra (MS) were recorded using a MS901 AEI spectrometer.

2-(4-Methoxy-phenyl)-benzimidazole-5-carboxylic acid ethyl ester (3). A mixture of 1,2-diaminobenzoic acid ethyl ester (1 g, 5.5 mmol) and anisaldehyde (0.67 mL, 5.5 mmol) in 25 mL of nitrobenzene was heated at 140 °C. Thirty-six hours later, an additional portion of anisaldehyde (0.2 mL, 1.6 mmol) was added and the heating was continued for another 5 h. After the removal of nitrobenzene under reduced pressure, the crude compound was purified by flash chromatography over silica gel (AcOEt/hexane: 4/6–5/5). The desired compound **3** (1.06 g) was obtained in 65% yield. ^{1}H NMR ($CDCl_3$): d 1.40 (t, 3H, CH_3, $J = 7.1$ Hz), 3.84 (s, 3H, OCH_3), 4.40 (q, 2H, CH_2, $J = 7.1$ Hz), 6.95 (d, 2H, ArH, $J = 8.9$ Hz), 7.61 (d, 1H, ArH, $J = 8.4$ Hz), 7.98 (dd, 1H, ArH, $J_1 = 8.4$ Hz, $J_2 = 1.6$ Hz), 8.05 (d, 2H, ArH, $J = 8.8$ Hz, 8.83 (d, 1H, ArH, $J = 1.6$ Hz). MS: 296 (100, M^+). Anal. calcd for $C_{17}H_{26}N_2O_3$ (296.326): C 68.91, H 5.44, N 9.45; found: C 69.13, H 5.59, N 8.87.

[2-(4-Methoxy-phenyl)-1″H″-benzimidazole-5-yl]-methanol (4). Under argon, to a solution of compound **3** (297 mg, 1 mmol) in dry THF (20 mL), $LiAlH_4$ (140 mg, 3.7 mmol) was added and the mixture was stirred for

8 h. Another portion of $LiAlH_4$ (116 mg, 3 mmol) was added and the reaction mixture was heated to reflux for overnight. After cooling to room temperature, the reaction mixture was poured carefully to a NH_4Cl saturated solution (5 mL) and further acidified to pH 4 with 4 N HCl. After introducing 5 mL of MeOH and Speedex, the mixture was stirred for another 30 min and filtered. The filtrate was concentrated under vaccum and the obtained residue was purified by chromatography over silica gel (CH_2Cl_2/CH_3OH: 95/5), to afford the title compound **4** (171 mg, 67%). ^1H NMR (MeOH-d_4): 3.87 (s, 3H, OCH_3), 4.72 (S, 2H, $HOCH_2$), 7.08 (d, 2H, ArH, $J=8.9$ Hz), 7.25 (dd, 1H, ArH, $J_1=8.4$ Hz, $J_2=1.6$ Hz), 7.55 (d, 1H, ArH, $J=8.4$ Hz), 7.60 (d, 1H, ArH, $J=1.6$ Hz), 8.02 (d, 1H, $J=8.9$ Hz). MS: 254 (100, M^+), 237 (40, M^+-OH), 225 (46, M^+-CH_2OH).

[2-(4-Methoxy-phenyl)-1″H″-benzimidazole-5-carb-aldehyde (5). Method A. A mixture of alcohol **4** (800 mg, 3.2 mmol) and active manganese dioxide (1600 mg, 18.4 mmol) in CH_2Cl_2 (50 mL) and DMF (10 mL) was stirred at 60 °C for 3 days. After cooling to room temperature, the mixture was filtered through a bed of Speedex. The filtrate was concentrated under reduced pressure and the resulting residue was purified by chromatography over silica gel (CH_2Cl_2/CH_3OH: 100/0–90/10). The aldehyde (720 mg, 93%) was obtained as a beige solid. The alcohol **4** could be also transformed to aldehyde **5** by oxidation with three equivalents of pyridium chlorochromate in CH_2Cl_2 at room temperature, in about 50% yield.

Method B. To a solution of compound **7** (5.9 g, 19 mmol) in 200 mL of THF/Et_2O (3/1), $LiAlH_4$ (2.1 g, 57 mmol) was added in small portion at −70 °C. The stirring was continued for 6 h and the reaction temperature was kept below −20 °C. The reaction was quenched by carefully introducing of AcOEt (100 mL) to destroy the excess of $LiAlH_4$ and the temperature was allowed to raise to room temperature. The mixture was then acidified to pH ~5 with 12.5 N HCl/MeOH solution, followed by addition of NH_4Cl saturated solution (30 mL). After 15 min stirring, Speedex powder was added to the mixture and the stirring was continued for another 30 min. Finally, the mixture was filtered and the filtrate was concentrated under reduced pressure. The residue was purified by flash chromatography over silica gel to give the desired aldehyde **5** (4.25 g, 88%). ^1H NMR (DMSO-d_6): 3.86 (s, 3H, OCH_3), 7.15 (d, 2H, ArH, $J=8.9$ Hz), 7.75 (dd, d, 2H, ArH), 8.14 (d, 1H, ArH, $J=8.4$ Hz), 8.17 (d, 2H, ArH, $J=8.9$ Hz). MS: 252 (100, M^+). Anal. calcd for $C_{15}H_{12}N_2O_2$ (252.273): C 71.42, H 4.79, N 11.10; found: C 71.22, H 4.85, N 10.90.

***N*-Methoxy-*N*-methyl-3,4-dinitrobenzamide (6).** A mixture of 3,4-dinitrobenzoic acid (20 g, 94 mmol) and $SOCl_2$ (55 mL) was heated at 80 °C for 4 h and then concentrated under reduced pressure. Dry toluene was added to the resulting residue and evaporated to dryness, such procedure was repeated three times. Finally, the acid chloride was obtained as a yellow solid (21.7 g). ^1H NMR ($CDCl_3$): 8.06 (d, 1H, ArH, $J=8.4$ Hz), 8.52 (dd, 1H, $J_1=8.5$ Hz, $J_2=1.9$ Hz), 8.71 (d, 1H, ArH, $J=1.9$ Hz). Anal. calcd for $C_7H_3ClN_2O_5$ (230.56): C 36.47, H 1.31, N 12.15; found: C 36.53, H 1.49, N 12.11.

The above acid chloride (20 g, 86 mmol) was dissolved in CH_2Cl_2 (150 mL) and the solution was cooled to 0 °C. After addition of pyridine (21 mL, 260 mmol) and *N*,*O*-dimethylhydroxylamine hydrochloride (12.6 g, 129 mmol), the ice-bath was removed and the mixture was stirred overnight at room temperature. The reaction mixture was diluted with 200 mL of CH_2Cl_2 and the organic layer was washed twice with brine, dried over Na_2SO_4 and concentrated. The crude compound was purified by flash chromatography over silical gel (AcOEt/hexane: 1/1–8/2), to fournish the title compound **6** (20.3 g, 92%) as an orange solid. ^1H NMR ($CDCl_3$): 3.43 (s, 3H, CH_3), 3.59 (S, 3H, CH_3), 7.96 (d, 1H, ArH, $J=8.4$ Hz), 8.11 (dd, 1H, ArH, $J_1=8.4$ Hz, $J_2=1.9$ Hz), 8.31 (d, 1H, ArH, $J=1.9$ Hz). MS: 255 (8, M^+), 195 (100, M^+-MeNOMe). Anal. calcd for $C_9H_9N_3O_6$ (255.186): C 42.36, H 3.56, N 16.47; found: C 42.33, H 3.63, N 16.42.

[2-(4-methoxy-phenyl)-1″H″-benzimidazole-5-carboxylic acid methoxy-methylamide (7)

Method I: Coupling in nitrobenzene. A solution of methoxy methyl 3,4-dinitrobenzoic amide **6** (2 g, 7.8 mmol) was hydrogenated over 5% Pd/C (800 mg) in EtOH (200 mL) at room temperature for 3 h, to give *N*-methoxy *N*-methyl 3,4-diaminobenzoic amide. After hydrogenation, 50 mL of nitrobenzene was added and EtOH was removed under reduced pressure. After addition of another 50 mL of nitrobenzene and anisaldehyde (0.95 mL, 7.8 mmol), the mixture was stirred at 140 °C for 24 h, then cooled to room temperature and filtered to remove the catalyst. The filtrate was concentrated under reduced pressure and resulting residue was loaded on a column of silica gel, which was eluted with AcOEt/MeOH (100/0–98/2) and give the desired benzimidazole **7** (1.7 g) in 69% yield.

Method II: Coupling with $Na_2S_2O_5$. After hydrogenation, a solution of $Na_2S_2O_5$ (770 mg, 4 mmol) in H_2O (1.6 mL) was introduced directly to the mixture, followed by addition of anisaldehyde (0.98 mL, 8 mmol). The resulting mixture was stirred at reflux for 4 h, then cooled to room temperature and filtered through a bed of Speedex. The filtrate was concentrate under reduced pressure and the obtained residue was purified by chromatography to furnish 1.95 g of the title compound **7** in 80% yield. ^1H NMR ($CDCl_3$): 3.40 (s, 3H, CH_3), 3.57 (S, 3H, CH_3), 3.82 (s, 3H, OCH_3), 6.91 (d, 2H, ArH, $J=8.9$ Hz), 7.56 (m, 2H, ArH), 7.93 (s, broad, 1H, ArH), 8.06 (d, 2H, ArH, $J=8.9$ Hz). MS: 311 (5, M^+), 251 (100, M^+-N(OCH3)CH3). Anal. calcd for $C_{17}H_{17}N_3O_3$ (311.34): C 65.58, H 5.50, N 13.50; found: C 65.40, H 5.72, N 13.71.

2′-(4-Methoxy-phenyl)-[2,5′] bisbenzoimidazole-5-carboxylic acid (8). To a mixture of 3,4-diaminobenzoic acid (2.3 g, 15 mmol) and aldehyde **5** (3.8 g, 15 mmol) in EtOH (250 mL), 50 mL of solution of sodium pyro-

sulfite (1.5 g, 8 mmol) was added and the mixture was heated to reflux overnight. After cooling to room temperature, 100 mL of H_2O was added to the reaction mixture and resulting precipitate was filtered. The obtained solid was recrystalized in MeOH to give the title compound **8** (4.1 g, 71%) as brown solid. ^{1}H NMR (DMSO-d_6): 3.89 (s, 3H, CH_3), 7.24 (d, 2H, ArH, $J=8.9$ Hz), 7.78 (d, 1H, ArH, $J=8.5$ Hz), 7.90 (d, 1H, ArH, $J=9.0$ Hz), 7.95 (dd, 1H, ArH, $J_1=8.5$ Hz, $J_2<2$ Hz), 8.22 (d, 2H, ArH, $J=8.9$ Hz), 8.24 (dd and d, 2H, ArH), 8.49 (d, 1H, ArH, $J<2$ Hz). MS (ISP): 385 (100, MH^+).

2′-(4-Methoxy-phenyl)-[2,5′] bis-benzoimidazole-5-carboxylic acid methoxy-methyl amide (9). A mixture of **8** (1.1 g, 2.2 mmol) and $SOCl_2$ (1.1 mL, 15 mmol) was refluxed for 4 h, then concentrated under reduced pressure and further coevaporated twice with toluene (2×100 mL). After drying under vaccuum, the obtained residue was dissolved in CH_2Cl_2 (100 mL) and *N*,*O*-dimethylhydroxyamine hydrochloride (0.44 g, 4.5 mmol) and pyridine (0.8 mL, 10 mmol) were added. The mixture was stirred at room temperature for 24 h and the usual work up was followed. The crude product was purified by chromatography over silica gel with CH_2Cl_2/MeOH as eluent, to give title compound **9** (560 mg, 47%) as beige solid (47%). ^{1}H NMR (DMSO-d_6): 3.31 (s, 3H, NCH_3), 3.59 (s, 3H, $NOCH_3$), 3.86 (s, 3H, OCH_3), 7.15 (d, 2H, ArH, $J=8.8$ Hz), 7.49 (dd, 1H, ArH, $J_1=8.3$ Hz, $J_2<2$ Hz), 7.63 (d, 1H, ArH, $J=8.3$ Hz), 7.72 (d, 1H, ArH, $J=8.5$ Hz), 7.88 (d, 1H, ArH, $J<2$ Hz), 8.08 (dd, 1H, ArH, $J_1=8.5$ Hz, $J_2<2$ Hz), 8.17 (d, 2H, ArH, $J=8.8$ Hz), 8.38 (d, 1H, ArH, $J<2$ Hz), 13.08 (broad, 2H, NH). MS (ISP): 428 (100, $M+H^+$).

2′-(4-Methoxy-phenyl)-[2,5′] bis-benzimidazole-5-carbaldehyde (10). To a suspension of **9** (427 mg, 1 mmol) in THF/Et_2O (30/20 mL), $LiAlH_4$ (150 mg, 3 mmol) was added at −70 °C. The mixture was stirred for 5 h and the temperature was allowed to raise to room temperature. The reaction was quenched by slow addition of AcOEt (50 mL) at 0 °C and then NH_4Cl saturated solution (15 mL). After 30 min further stirring at room temperature, the mixture was filtered through a bed of Speedex and the filtrate was concentrated under reduced pressure. The resulting residue was dissolved in MeOH and precipitated with Et_2O, to provide compound **10** (220 mg, 60%) as beige solid. ^{1}H NMR (DMSO-d_6): 3.89 (s, 3H, OCH_3), 7.22 (d, 2H, ArH, $J=8.9$ Hz), 7.82–7.89 (m, 3H, ArH), 8.21–8.27 (m, 2H, ArH), 8.27 (d, 2H, ArH, $J=8.9$ Hz), 8.54(d, 1H, ArH, $J<2$ Hz), 10.08 (s, 1H, CHO). MS (ISP): 369 (100, $M+H^+$).

5-(4-Methyl-1-piperazinyl)-2-nitroaniline (11). A mixture of 5-chloro-2-nitroaniline (34.2 g, 0.2 mol), *N*-methylpiperazine (22 g, 0.2 mol) and potasium carbonate (28 g, 0.2 mol) in DMF (100 mL) was heated at reflux for 3 h and then cooled to room temperature. After addition of 200 mL of H_2O, the resulting precipitate was filtered and the obtained solid was suspended in 1L of 2 N acetic acid and filtered. The filtrate was slightly basified with ammoniac solution and the resulting precipitate was filtered off to give the title compound **11** (38 g, 82%) as a yellow solid. ^{1}H NMR ($CDCl_3$): 2.21 (s, 3H, CH_3), 2.38–2.42 (m, 4H, $2CH_2$), 3.29–3.34 (m, 4H, $2CH_2$), 6.21 (d, 1H, ArH, $J=2.7$ Hz), 6.39 (dd, 1H, ArH, $J_1=2.7$ Hz, $J_2=9.8$ Hz), 6.27 (broad, 2H, NH_2), 7.80 (d, 1H, ArH, $J=9.8$ Hz). MS: 236 (46, M^+), 221 (10, $M-CH_3$), 165 (16, $M-C_4H_9N$), 70 (100, C_4H_8N). Anal. calcd for $C_{11}H_{16}N_4O_2$ (236.275): C 55.87, H 6.84, N 23.71; found: C 55.32, H 6.88, N 23.51.

[1-(3-amino-4-nitro-phenyl)-pyrrolidin-3-yl]-carbamic acid '*tert*'-butyl ester (12). A mixture of 5-chloro-2-nitroaniline (7.8 g, 46 mmol), 3-*tert*-butoxycarbonylamino-pyrrolidine (8.5 g, 45.6 mol) and potassium carbonate (6.4 g, 46.3 mol) in DMF (200 mL) was heated at reflux for 3 h and then cooled to room temperature. After addition of 200 mL of H_2O, the mixture was extracted with AcOEt (3×150 mL) and the organic layer was washed with brine, dried over anhydrous Na_2SO_4 and concentrated. The title compound **12** (13.3 g, 91%) was provided after purification by flash chromatography over silica gel (CH_2Cl_2/MeOH), as yellow solid. ^{1}H NMR ($CDCl_3$): 1.35 (s, 9H, $(CH_3)_3$), 2.01, 2.31 (2m, 2H, CH_2), 3.24 (dd, 1H, CH_2N, $J_2=4$ Hz, $J_2=11.6$ Hz), 3.47 (m, 1H, CH_2N), 3.66 (dd, 1H, $J_1=5.2$ Hz, $J_2=11.6$ Hz), 4.36 (m, 1H, CH), 4.71 (broad, 1H, NH), 5.60 (d, 1H, ArH, $J=2.4$ Hz), 6.02 (dd, 1H, ArH, $J_1=2.4$ Hz, $J_2=9.5$ Hz), 6.18 (broad, 2H, NH_2), 8.02 (d, 1H, ArH, $J=9.5$ Hz). MS: 322 (10, M^+), 249 (10, M^+-tBuO), 205 (100, M^+-BocNH$_2$). Anal. calcd for $C_{15}H_{22}N_4O_4$ (322.365): C 55.89, H 6.88, N 17.38; found: C 55.88, H 6.94, N 16.95.

1-{2′-(4-methoxy-phenyl)-[2,5′]bibenzimidazol-5-yl}-pyrrolidin-3-ylamine (1b). A solution of compound **12** (1162 g, 3.6 mmol) in EtOH (200 mL) was hydrogenated over 5% Pd/C (600 mg) at room temperature for 2 h. After hydrogenation, aldehyde **5** (759 g, 3.0 mmol) and 3 mL of aqueous solution of sodium pyrosulfite (286 mg, 1.5 mmol) in H_2O were added. The mixture was stirred at reflux for 5 h and then cooled to room temperature, filtered to remove catalyst. The filtrate was concentrated under reduced pressure and purified by chromatography over Florisil (AcOEt/MeOH: 100/0–90/10), to provide the bis-benzimidazole with NH_2-protected by Boc group (1128 mg), in 81% yield. ^{1}H NMR (400 Hz, DMSO-d_6): 1.41 (s, 9H, $(CH_3)_3C$), 1.87–1.97 (m, 1H, CH_2), 2.16–2.25 (m, 1H, CH_2), 3,10 (m, 1H, CH_2N), 3.24–3.56 (3m, 3H, CH_2N), 3.86 (s, 3H, OCH_3), 4.17 (m, 1H, CHN), 6.55 (m, 2H, ArH), 7.14 (d, 2H, ArH, $J=8.7$ Hz), 7.21 (d, 1H, ArH), 7.42 (d, 1H, ArH, $J=8.5$ Hz), 7.66 (broad, 1H, ArH or NHCO), 7.99 (d, 1H, ArH), 8.16 (d, 2H, ArH, $J=8.7$ Hz), 8.26 (broad, 1H, ArH or NHCO), 12.95 (broad, 2H, NH). MS: 424 (86, MH^+-Boc). Anal. calcd for $C_{30}H_{32}N_6O_3$ (524.62) containing 2.03% of water: C 67.92, H 6.15, N 16.02; found: C 68.38, H 6.31, N 15.76.

The Boc protecting group was removed as follows: 503 mg of above compound was dissolved in CH_2Cl_2 (20 mL) at 0 °C and trifluoroacetic acid (10 mL) was added. The mixture was stirred for 2 h and the temperature was allowed to raise to room temperature.

Afterwards, the mixture was evaporated to dryness and was purified by reverse phase chromatography over a Opti-up column with CH_3CN/H_2O (containing 0.4% TFA) as eluent. The collected fractions were concentrated under reduced pressure to remove CH_3CN and then lyophilized to afford the bis-benzimidazole **1b** as orange powder in 81% yield. ^{1}H NMR (400 Hz, DMSO-d_6): 2.19–2.20 (m, 1H, CH_2), 2.36–2.47 (m, 1H, CH_2), 3.37–3.47 (m, 2H, CH_2N), 3.54–3.69 (2m, 2H, CH_2N), 3.87 (s, 3H, OCH_3), 3.99–4.19 (m, 1H, CHN), 6.73 (d, 1H, ArH, $J<2$ Hz), 6.90 (dd, 1H, ArH, $J_1=8.5$ Hz, $J_2<2$ Hz), 7.18 (d, 2H, ArH, $J=8.8$ Hz), 7.66 (d, 1H, ArH, $J=8.9$ Hz), 7.87 (d, 1H, ArH, $J=8.5$ Hz), 8.00 (dd, 1H, ArH, $J_1=8.9$ Hz, $J_2<2$ Hz), 8.16 (m, 3H, NH_3^+), 8.20 (d, 2H, ArH, $J=8.8$ Hz), 8.42 (d, 1H, ArH, $J<2$ Hz), 14.75 (broad, 2H, NH). MS (ISP): 425 (100, MH^+). Anal. calcd for $C_{25}H_{24}N_60_1$•2.95 mol CF_3COOH•3.4 mol H_2O (822.14): C 45.14, H 4.14, N 10.22, F 20.45, H_2O 7.45; found: C 45.50, H 3.93, N 10.32, F 20.75, H_2O 7.93.

1-{2″-(4-Methoxy-phenyl)-[2,5′:2′,5″]terbenzimidazole-5-yl}-pyrrolidin-3-ylamine (2b). Tris-benzimidazole **2b** was synthesized in a similar manner as bisbenzoimidazole **1b**. A solution of compound **12** (322 mg, 1 mmol) in EtOH (100 mL) was hydrogenated over 5% Pd/C (100 mg) at room temperature for 3 h. After hydrogenation, aldehyde **10** (352 mg, 1 mmol) and 1 mL of solution of sodium pyrosulfite (100 mg, 0.52 mmol) were added. The mixture was stirred at reflux overnight, then cooled to room temperature, filtered to remove catalyst. The filtrate was concentrated under reduced pressure to obtain a brown solid, which was purified by reverse phase chromatography over an Opti-up column with CH_3CN/H_2O (containing 0.1% TFA) as eluent. The collected fractions were concentrated under reduced pressure to remove CH_3CN and then lyophilized, to afford tris-benzimidazole with NH_2-protected by Boc group (99 mg, 59%), as orange solid.

The Boc protecting group was removed by treatment with trifluoroacetic acid (4 mL) in CH_2Cl_2 (8 mL), from 0 °C to room temperature. After deprotection, the mixture was evaporated to dryness and the crude product was purified by HPLC reverse phase chromatography over RP-18 Select-B column with CH_3CN/H_2O (containing 0.4% TFA) as eluent. The collected fractions were concentrated under reduced pressure and lyophilized to afford the title tris-benzoimidazole **2b** as orange solid, in 59% yield. ^{1}H NMR (400 Hz, DMSO-d_6): 2.14 (m, 1H, CH_2), 2.41 (m, 1H, CH_2), 3.37–3.47 (m, 2H, CH_2N), 3.54–3.69 (2m, 2H, CH_2N), 3.88 (s, 3H, OCH_3), 4.18 (m, 1H, NCH), 6.73 (d, 1H, ArH, $J<2$ Hz), 6.90 (dd, 1H, ArH, $J_1=8$–9 Hz, $J_2<2$ Hz), 7.29 (d, 2H, ArH, $J=8.8$ Hz), 7.67 (d, 1H, ArH, $J=8.5$ Hz), 7.80 (d, 1H, ArH, $J=8.5$ Hz), 7.91 (d, 1H, ArH, $J=8.5$–9 Hz), 8.03 (dd, 1H, ArH, $J_1=8$–9 Hz, $J_2<2$ Hz), 8.13 (m, NH_3^+ or NH^+), 8.18 (dd, 1H, ArH), 8.20 (d, 2H, ArH, $J=8.8$ Hz), 8.48 (broad, 2H, ArH). MS (ISP): 541 (100, MH^+).

2″-(4-methoxy-phenyl)-6-(4-methylpiperazin-1-yl)-[2,5′;2′,5″]tertbenzimidazole (2a). 5-(*N*-Methylpiperazinyl)-2-nitroaniline **11** (236 mg, 1 mmol) was hydrogenated over 5% Pd/C (100 mg) in EtOH (50 mL). After hydrogenation, 5 mL solution of $Na_2S_2O_5$ (100 mg, 0.53 mmol) and aldehyde **10** (500 mg, 1.5 mmol) were introduced. The mixture was stirred at reflux overnight and then filtered. After addition of 100 mL of H_2O into the filtrate, the resulting precipitates were collected and recrystallized in MeOH to give the title tris-benzimidazole **2a** (120 mg, 21.7%), which was transformed to the hydrochloride salt by HCl/MeOH solution. The low yield was due to the purification step. ^{1}H NMR (DMSO-d_6): 2.87 (s, 3H, NCH_3), 3.20–3.51 (m, 8H, CH_2N), 3.87 (s, 3H, OCH_3), 7.01 (dd, 1H, ArH, $J_1=8.8$ Hz, $J_2<2$ Hz), 7.14 (d, 1H, ArH, $J<2$ Hz), 7.16 (d, 2H, ArH, $J=8.8$ Hz), 7.52 (d, 1H, ArH, $J=8.7$ Hz), 7.67–7.80 (m, 2H, ArH), 8.06 (d, 1H, ArH, $J=8.5$–9 Hz), 8.12 (d, 1H, ArH, $J=8$–9 Hz), 8.18 (d, 2H, $J=8.8$ Hz), 8.35–8.45 (m, 2H, ArH), 13.08 (broad, 2–3H, NH). MS (ISP): 555 (100, $M+H^+$). Anal. calcd for $C_{33}H_{30}N_8O_1$•3.8 mol HCl (693.210) containing MeOH (2.78%): C 56.63, H 5.13, N 15.72, Cl 18.90; found: C 56.61, H 5.18, N 15.41, Cl 19.00.

Chemicals and biochemicals

Hoechst 33258 and Hoechst 33342 were purchased from Sigma Chemical Co. (UK) Stock solutions were prepared in water before subsequent dilution with a 10 mM Tris–HCl buffer pH 7.0, containing 10 mM NaCl. Ammonium persulphate, tris base, acrylamide, bis-acrylamide, ultrapure urea, boric acid, tetramethylethylenediamine and dimethyl sulphate were from BDH. Formic acid, piperidine, hydrazine and formamide were from Aldrich. Photographic requisites were from Kodak. Bromophenol blue and xylene cyanol were from Serva. α-[^{32}P]-dATP was obtained from NEN Dupont. Unlabeled dATP was ultra-pure grade from Pharmacia. Restriction endonucleases *Ava*I, *Eco*RI and *Pvu*II (Boehringer Mannheim, Germany) were used according to the supplier's recommended protocol in the activity buffer provided. Avian myeloblastosis virus (AMV) reverse transcriptase was from Pharmacia. Plasmids pKMΔ-98, pUC12 and pBS (Stratagene, La Jolla, CA, USA) were isolated from *Escherichia coli* by a standard sodium dodecyl sulphate–sodium hydroxide lysis procedure and purified by banding in CsCl–ethidium bromide gradients. Ethidium was removed by several isopropanol extractions followed by exhaustive dialysis against tris–EDTA buffer. The purified plasmid was then precipitated and resuspended in appropriate buffer prior to digestion by the restriction enzymes. All other chemicals were analytical grade reagents, and all solutions were prepared using doubly deionised, Millipore filtered water.

Melting temperature studies

Absorption spectra were recorded on a Uvikon 943 spectrophotometer. The 12-cell holder was thermostated with a Neslab RTE 111 cryostat. Drug-RNA complexes were prepared by adding aliquots of a concentrated drug solution to a DNA solution at constant concentration (usually 20 μM) in BPE buffer pH 7.1 (6 mM Na_2HPO_4, 2 mM $Na_2H_2PO_4$, 1 mM EDTA). A heating rate of 1 °C/min was used and data points were collected

every 30 s. The temperature inside the cuvette was monitored by using a thermocouple. The absorbance at 260 nm was measured over the range 25–90 °C in 1-cm path length reduced volume quartz cells. The 'melting' temperature T_m was taken as the mid-point of the hyperchromic transition determined from first derivatives plots. The reproducibility of the *T*m measurements was ±1 °C.

Linear dichroism measurements

Flow-oriented linear dichroism (LD) spectra were recorded in a Couette cell using the experimental setup previously described.[41]

DNA restriction fragments

Three DNAs of different base composition: (i) a 117 bp DNA fragment from plasmid pBS, (ii) the 160 bp *tyr* T DNA fragment and (iii) a 178 bp DNA fragment from plasmid pUC12 were used in the DNAaseI footprinting studies. The *tyr* T DNA was obtained by digestion of the plasmid pKMΔ-98 with *Eco*RI and *Ava*I.[53] The 117 mer and 178 mer were obtained after digestion of the corresponding plasmid with the restriction enzymes *Pvu*II and *Eco*RI. In each case, the fragment was incubated with AMV reverse transcriptase in the presence of α-[^{32}P]-dATP to label specifically the 3′-end at the *Eco*RI site. The singly end-labeled DNA fragment was then purified by preparative non-denaturing polyacrylamide gel electrophoresis (6.5% acrylamide, 1.5 mm thick, 200 V, 2 h, in TBE buffer: 89 mM Tris base, 89 mM boric acid, 2.5 mM Na_2 EDTA, pH 8.3). After rapid autoradiography to locate the DNA, the band was excised from the gel, minced with a blade and extracted overnight in 500 mM ammonium acetate, 10 mM magnesium acetate. The purified DNA was then precipitated twice with 70% ethanol prior to resuspension in 10 mM Tris, 10 mM NaCl buffer pH 7.0.

DNase I footprinting

These experiments were performed essentially according to a published protocol.[54] Reactions were conducted in a total volume of 8 μL. Samples (2 μL) of the labeled DNA fragment were incubated with 4 μL of the buffer solution containing the ligand at appropriate concentration. After 30–60 min incubation at 37 °C to ensure equilibration of the binding reaction, the digestion was initiated by the addition of 2 μL of a DNAase I solution whose concentration was adjusted to yield a final enzyme concentration of about 0.01 unit/mL in the reaction mixture. The extent of digestion was limited to less than 30% of the starting material so as to minimize the incidence of multiple cuts in any strand ('single-hit' kinetic conditions). Optimal enzyme dilutions were established in preliminary calibration experiments. After 3 min, the digestion was stopped by freeze drying, samples were lyophilized, washed once with 50 μL of water, lyophilized again and then resuspended in 4 μL of an 80% formamide solution containing tracking dyes. Samples were heated at 90 °C for 4 min and chilled in ice for 4 min prior to electrophoresis.

Electrophoresis and autoradiography

DNA cleavage products were resolved by polyacrylamide gel electrophoresis under denaturing conditions (0.3 mm thick, 8% acrylamide gels containing 8 M urea) capable of resolving DNA fragments differing in length by one nucleotide. Electrophoresis was continued until the bromophenol blue marker had run out of the gel (about 2.5 h at 60 Watts, 1600 V in TBE buffer; BRL sequencer Model S2). Gels were soaked in 10% acetic acid for 15 min, transferred to Whatman 3MM paper, dried under vacuum at 80 °C, and subjected to autoradiography at −70 °C with an intensifying screen. Exposure times of the X-ray films (Fuji R-X) were adjusted according to the number of counts per lane loaded on each individual gel (usually 24 h).

Quantitation by storage phosphor imaging

A Molecular Dynamics 425E PhosphorImager was used to collect data from storage screens exposed to dried gels overnight at room temperature. Base line-corrected scans were analyzed by integrating all the densities between two selected boundaries using ImageQuant version 3.3 software. Each resolved band was assigned to a particular bond within the DNA fragment by comparison of its position relative to sequencing standards generated by treatment of the DNA with formic acid (G + A) followed by piperidine-induced cleavage at the modified bases in DNA.

Acknowledgements

This work was done under the support of research grants (to C.B.) from the Ligue Nationale Française contre le Cancer, Comité du Nord and (to M.J.W.) from the European Union, the Wellcome Trust, CRC and AICR. The authors thank the Sir Halley Stewart Trust for a grant to assist cooperation.

References and Notes

1. Stokke, T.; Steen, H. B. *J. Histochem. Cytochem.* **1985**, *33*, 333.
2. Hauglang, R. P. In *Handbook of Fluorescent Probes and Research Chemicals*, 6th ed.; Spence, M. T. Z., Ed.; Molecular Probes: Eugene, OR, 1996.
3. Portugal, J.; Waring, M. J. *Biochim. Biophys. Acta* **1987**, *949*, 158.
4. Pjura, P. E.; Grzeskoniak, K.; Dickerson, R. E. *J. Mol. Biol.* **1987**, *197*, 257.
5. Kopka, M. L.; Pjura, P.; Goodsell, D.; Dickerson, R. E. In *Nucleic Acids and Molecular Biology*; Eckstein, F.; Lilley, D. M. J., Eds.; Springer: Berlin, 1987; Vol. 1, pp 1–24.
6. Jorgenson, K. F.; Varshney, U.; van de Sande, J. H. *J. Biomol. Struct. Dyn.* **1988**, *5*, 1005.
7. Loontiens, F. G.; Regenfuss, P.; Zechel, A.; Dumortier, L.; Clegg, R. M. *Biochemistry* **1990**, *29*, 9029.
8. Loontiens, F. G.; McLaughlin, L. W.; Diekmann, S.; Clegg, R. M. *Biochemistry* **1991**, *30*, 182.
9. Quintana, J. R.; Lipanov, A. A.; Dickerson, R. E. *Biochemistry* **1991**, *30*, 10294.

10. Sriram, M.; van der Marel, G. A.; Roelen, H. L. P. F.; van Boom, J. H.; Wang, A. H.-J. *EMBO J*. **1992**, *11*, 225.
11. Carrondo, M. A. A.deC.T.; Coll, M.; Aymami, J.; Wang, A. H. J.; Van der Marel, G. A.; Van Boom, J. H.; Rich, A. *Biochemistry* **1989**, *28*, 7849.
12. Searle, M. S.; Embrey, K. J. *Nucleic Acids Res*. **1990**, *18*, 3753.
13. Embrey, K. J.; Searle, M. S.; Craik, D. J. *J. Chem. Soc., Chem. Commun*. **1991**, 1770.
14. Embrey, K. J.; Searle, M. S.; Craik, D. J. *Eur. J. Biochem*. **1993**, *211*, 437.
15. Fede, A.; Labhardt, A.; Bannwarth, W.; Leupin, W. *Biochemistry* **1991**, *30*, 11377.
16. Parkinson, J. A.; Barber, J.; Douglas, K. T.; Rosamond, J.; Sharples, D. *Biochemistry* **1990**, *29*, 10181.
17. Parkinson, J. A.; Barber, J.; Douglas, K. T.; Rosamond, J.; Sharples, D. *Biochemistry* **1994**, *33*, 8442.
18. Vega, M. C.; Garcia Saez, I.; Aymami, J.; Eritja, R.; Van der Marel, G. A.; van Boom, J. H.; Rich, A.; Coll, M. *Eur. J. Biochem*. **1994**, *222*, 721.
19. Gavathiotis, E.; Sharman, G. J.; Searle, M. S. *Nucleic Acids Res*. **2000**, *28*, 728.
20. Fede, A.; Billeter, M.; Leupin, W.; Wüthrich, K. *Structure* **1993**, *1*, 177.
21. Haq, I.; Ladbury, J. E.; Chowdhry, B. Z.; Jenkins, T. C.; Chaires, J. B. *J. Mol. Biol*. **1997**, *271*, 244.
22. Czarny, A.; Boykin, D. W.; Wood, A. A.; Nunn, C. M.; Neidle, S.; Zhao, M.; Wilson, W. D. *J. Am. Chem. Soc*. **1995**, *117*, 4716.
23. Wood, A. A.; Nunn, C. M.; Czarny, A.; Boykin, D. W.; Neidle, S. *Nucleic Acids Res*. **1995**, *23*, 3678.
24. Clark, G. R.; Boykin, D. W.; Czarny, A.; Neidle, S. *Nucleic Acids Res*. **1997**, *25*, 1510.
25. Bostock-Smith, C. E.; Embrey, K. J.; Searle, M. S. *Nucleic Acids Res*. **1998**, *26*, 1660.
26. Ebrahimi, S. E. S.; Parkinson, J. A.; Fox, K. R.; McKie, J. H.; Barber, J.; Douglas, K. T. *J. Chem. Soc., Chem. Commun*. **1992**, 1398.
27. Clark, G. R.; Gray, E. J.; Neidle, S.; Ji, Y.-H.; Leupin, W. *Biochemistry* **1996**, *35*, 13745.
28. Bathini, Y.; Rao, K. E.; Shea, R. G.; Lown, J. W. *Chem. Res. Toxicol*. **1990**, *3*, 268.
29. Rao, K. E.; Lown, J. W. *Chem. Res. Toxicol*. **1991**, *4*, 661.
30. Kumar, S.; Joseph, T.; Singh, M. P.; Bathini, Y.; Lown, J. W. *J. Biomol. Struct. Dyn*. **1992**, *8*, 331.
31. Singh, M. P.; Joseph, T.; Kumar, S.; Bathini, Y.; Lown, J. W. *Chem. Res. Toxicol*. **1992**, *5*, 597.
32. Spink, N.; Brown, D. G.; Skelly, J. V.; Neidle, S. *Nucleic Acids Res*. **1994**, *22*, 1607.
33. Satz, A. L.; Bruice, T. C. *J. Am. Chem. Soc*. **2001**, *123*, 2469.
34. Gerber, P. R.; Müller, K. *J. Comput. Aided Mol. Des*. **1995**, *9*, 251.
35. Bathini, Y.; Lown, J. W. *Synthetic Commun*. **1990**, *20*, 955.
36. Nahm, S.; Weinreb, S. M. *Tetrahedron Lett*. **1981**, *22*, 3815.
37. Grimmet, M. R. In *Compressive Heterocyclic Chemistry*; Katritzky A. R.; Rees C. W., Eds.; 1984; Vol. 5, p 457.
38. Von Loewe, H.; Urbanietz, J. *Arzneim. Forsch*. **1974**, *24*, 1927.
39. Starshikov, N. M.; Pozharskii, A. F. *Khim. Chem. Heterocycl. Comp*. **1980**, 81.
40. Maquestiau, A.; Berte, L.; Mayence, A.; Vanden Eynde, J.-J. *Synthetic Commun*. **1991**, *21*, 2181.
41. Vogt, H.; Hänisch, G.; Hochstrasser, R. A. *Rev. Sci. Instrum*. **1995**, *66*, 4385.
42. Aymami, J.; Nunn, C. M.; Neidle, S. *Nucleic Acids Res*. **1999**, *27*, 2691.
43. Pilch, D. S.; Xu, Z.; Sun, Q.; LaVoie, E.; Liu, L. F.; Geacintov, N. E.; Breslauer, K. J. *Drug Des. Discov*. **1996**, *13*, 115.
44. Thurston, D. E.; Br, J. *Cancer* **1999**, *80*, 65.
45. Bailly, C.; Chaires, J. B. *Bioconjugate Chem*. **1998**, *9*, 513.
46. Drobyshev, A. L.; Zasedatelev, A. S.; Yershov, G. M.; Mirzabekov, A. D. *Nucleic Acids Res*. **1999**, *27*, 4100.
47. Sigman, D. S.; Chen, C.-H. B. *Annu. Rev. Biochem*. **1990**, *59*, 207.
48. Van Dyke, M. W.; Dervan, P. B. *Biochemistry* **1983**, *22*, 2373.
49. Suck, D.; Lahm, A.; Oefner, C. *Nature* **1988**, *332*, 465.
50. Weston, S. A.; Lahm, A.; Suck, D. *J. Mol. Biol*. **1992**, *226*, 1237.
51. Bailly, C.; Waring, M. J. *J. Biomol. Struct. Dyn*. **1995**, *12*, 869.
52. Clark, G. R.; Squire, C. J.; Gray, E. J.; Leupin, W.; Neidle, S. *Nucleic Acids Res*. **1996**, *24*, 4882.
53. Drew, H. R.; Travers, A. A. *Cell* **1984**, *37*, 491.
54. Low, C. M. L.; Drew, H. R.; Waring, M. J. *Nucleic Acids Res*. **1984**, *12*, 4865.